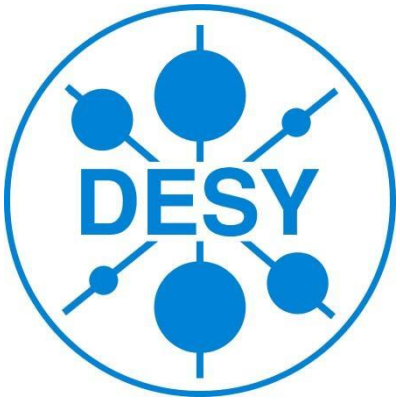

Fluorescence studies on mixing liquid jets

Dina Farrakhova
National Research Nuclear University “MEPhI”, Moscow, Russia

Supervisor:
Rita Graceffa
European XFEL, Hamburg, Germany
6 September, 2017

Abstract

This report describes studies of characterization of microfluidic device performance. Fluorescence quenching of Rhodamine 6G after mixing with potassium iodide allowed the determination of the mixing time of the device. By triggering the light source and the camera, it was possible to image twice a single Rhodamine B bead within the same frame and therefore to determine the jet speed. Combining the 2 parts of the study will allow to fully characterize the mixing jet that will be used at European XFEL.

Contents

1. **Introduction**

Proteins are complex, high-molecular organic compounds. They consist of amino acids and provide the vital processes performance of life forms [1]. X-ray crystallography allows determining structure and atom localization in different crystalline materials. The method is also used for studying dynamics of protein folding or enzymatic reactions [2-4].

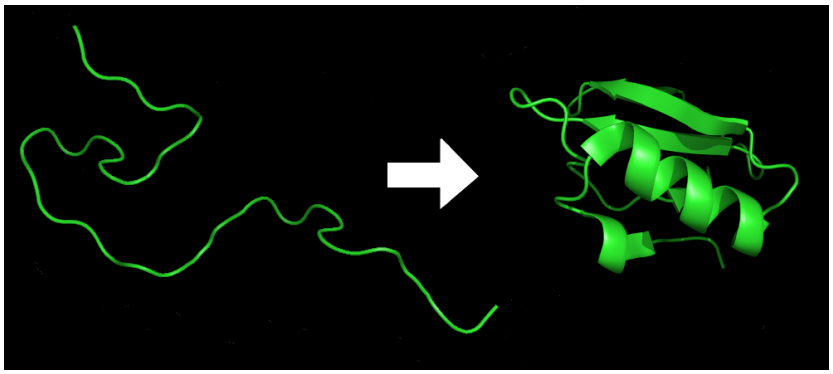

Figure 1. Protein before and after folding.

The structures of the transient states can be taken as basis for drug investigations [5]. Some chemical processes initiate reaction during the solutions mixing. The mixing time of liquid jet sets the time resolution of the structural measurements for a X-ray free electron laser (XFEL) experiments [2]. After that, femtosecond pulses of a XFEL determine characteristics of structure changing [2, 6, 7]. The characterization of devices producing mixing jet allows controlling mixing time and synchronizing it with the arrival time to the X-ray beam, where the diffusion has great significance [5].

Given the high-intensity beam produced by X-rays Free Electron Laser it is possible to study μm-size crystals. The protein sample is exposed ablation with subsequent high energy densities generation that transform rapidly into heat and kinetic energy [11]. The pulse width is so short, that diffraction images are taken before protein disruption, which describes properties and dynamics of matter [5]. The application of small size crystals (less than 10 μm) is important for performing time-resolved studies, because it allows to decreases the diffusion time of the substrate into the crystal [5, 8, 9]. If diffusion time exceeds protein turnover times, it enables to study protein conformation [10].

For X-ray crystallography experiments research samples is supplied like a jet via a Gas Dynamic Virtual Nozzle (GDVN). The GDVN device focuses liquid jet via flux of gas sheath with high pressure from central capillary [12-15]. This device fulfils conditions like avoiding clogging of nozzle and making thin jet for focusing X-ray beam, which diameter is about 1 micron [16].

The pre-selection of suitable values allow conducting successful further research of crystallized protein structural changing and gets valuable information on the function and dynamics of biomolecules.

2. Materials and methods

2.1. Chemical reagents. Micro particles based on melamine resin, carboxylate-modified, Rhodamine B-marked were purchased from Sigma-Aldrich.They present excellent monodispersity, and highly uniform spherical shape. 1, 5 and 10 µm beads size was used for experiments. The Rhodamine B confers fluorescence properties to the beads. Figure 2 shows their absorption and emission spectra, with maximum absorption at 560 nm and maximum emission at 584 nm.

Additional fluorescence experiments have been performed with aqueous solutions of Rhodamine 6G (Figure 3).

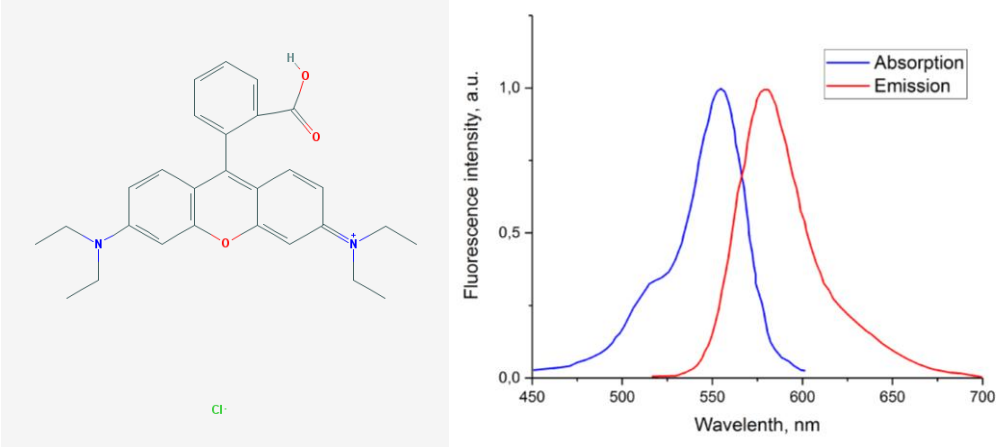

a) b)

Figure 2. a) Chemical structure of Rhodamine B, b) Absorption and emission spectra of Rhodamine B (λ_{Ex}= 560 nm, λ_{Em} = 584 nm).

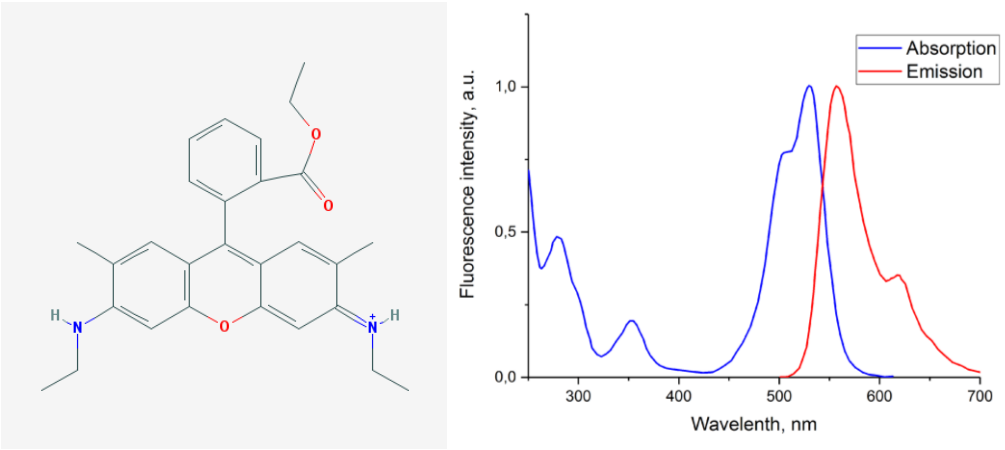

a) b)

Figure 3. a) Chemical structure of Rhodamine 6G, b) Absorption and emission spectra of Rhodamine 6G (λ_{Ex}= 530nm, λ_{Em} = 552 nm).

2.2. Installation. A MXP Valve (Rheodyne) was used for rapid solutions switching. It allows switching between 2- positions 6-ports (Fig.4).

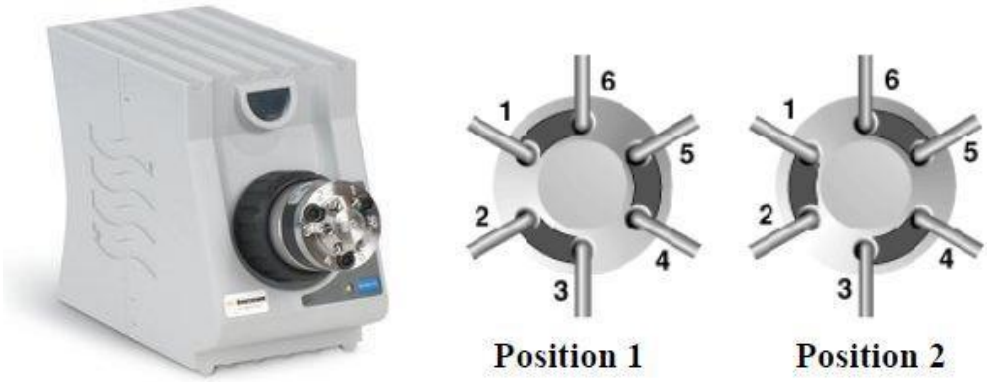

Figure 4. Scheme of switching valve positions.

The FASTCAM SA4 RV streak camera was used for registration image sequence of beads moving. It has mega pixel resolution, an ultra-sensitive image sensor capable of clear recording in low-light, and an ultra-high speed frame [17]. The SCHOTT Kaltlicht-Quelle KL 2500 LED white light source was used for bright-field microscopy illumination. The High-Power-LED, producing with extremely bright and non-coherent light, was used in pulsed and continuous mode for the fluorescence microscopy experiments.[18].

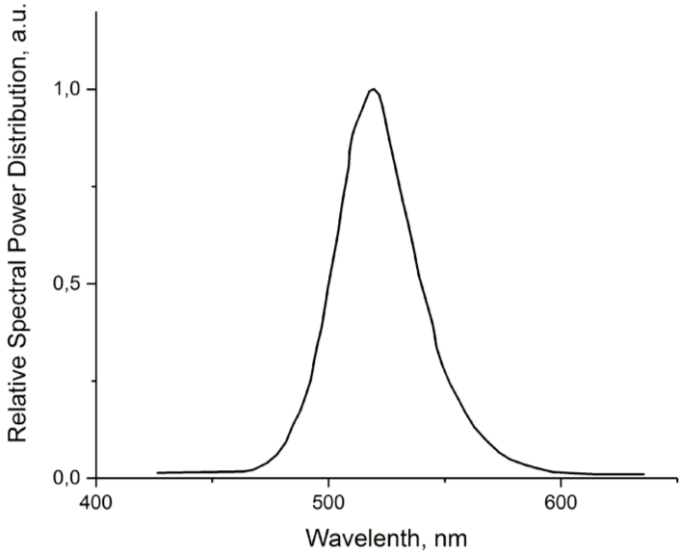

Figure 5. LED spectral characteristics.

The shortpass filter with diameter 25 mm (λ<550 nm) was placed after the LED and longpass filter with diameter 25 mm (λ<575 nm) (Fig.2) was placed before the camera lens to obtain fluorescence images, collecting exclusively the fluorescence of the Rhodamine molecules.. The values of the LED modes are summerized on the table 1 [18].

Continuous mode	Current, A	18
	Luminous flux, Im	2100
	Radiometric flux, W	4,1
Pulse mode	Current, A	250
	Luminous flux, Im	2
	Radiometric flux, W	14000

Table 1. Performance data of the LEDs

The LED double pulse mode was used for experiments on Rhodamine B beads (Fig..6). The trigger signal releases a double pulse with a break lasting 200,00±0,01 μs delay between the pulses. The width of the first and second pulses was 10 μs.

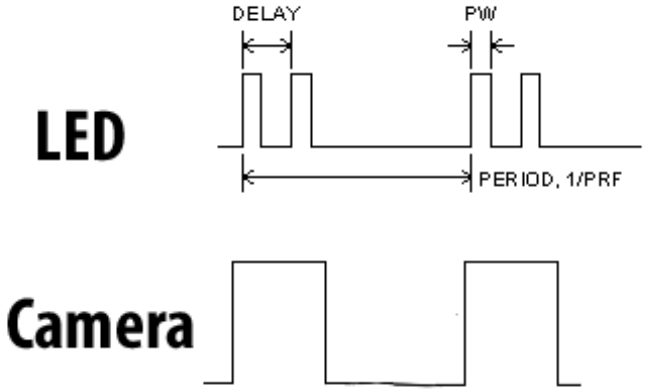

Figuree 6. The electrical signal of LED and camera.

A digital delay generator DG645 (Stanford Research Systems) synchronized the LED and the camera at a frequency of 50 Hz.. The Tektronix TDS 2024C oscilloscope was used for visualization of the electrical signal amplitude and time values. The liquid jet was produced with a glass nozzle. The syringe pump provided the continuous flowing rate of beads, also it allows to set dispensing volumes and inserts pauses, which increase quality of study operation. It holds 1 syringe with 2,5-20 cm^3 volume and the infusion flow rates were from

0,005 to 2.0 ml/min. Therefore, the small magnet was put to inside the syringe for supporting the stable concentration of colloidal suspension with beads. The camera calibration was conducted before the data analysis. The process involves calibrating a single image against known values (Fig.7), then applying that calibrated image to your unknown image with the same magnification [18].

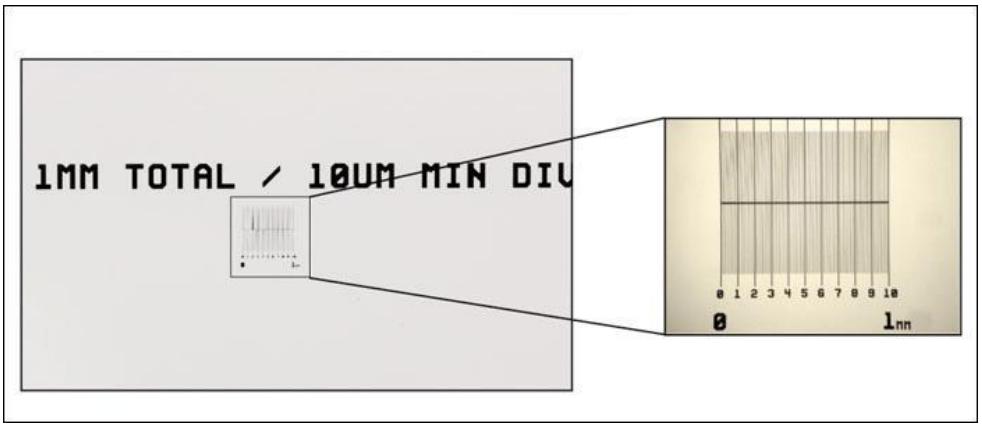

Figure 7. The stage micrometers image for calibration distance.

The scheme of set up is presented on the Figure 8.

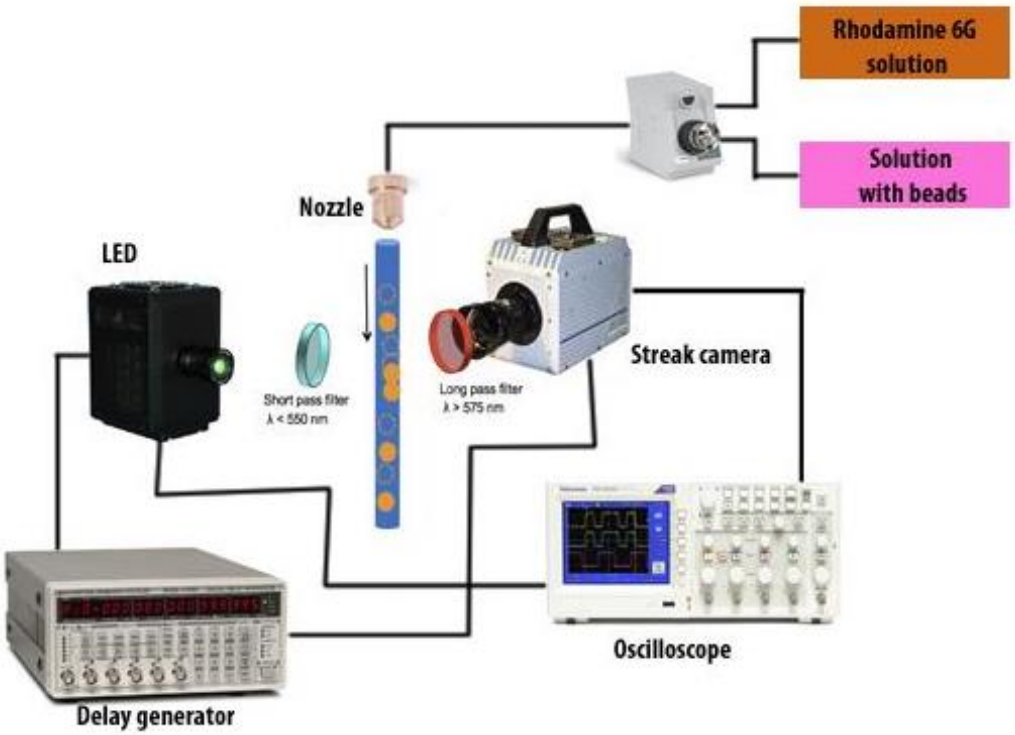

Figure 8. Set up scheme.

For mixing experiment, the a glass microfluidic device was used. There are 5 channels, the central channel is used for crystallized protein, two channels near the central channel are used for buffer, and the two last extreme channels are used for gas to form thin jet (Fig.9).

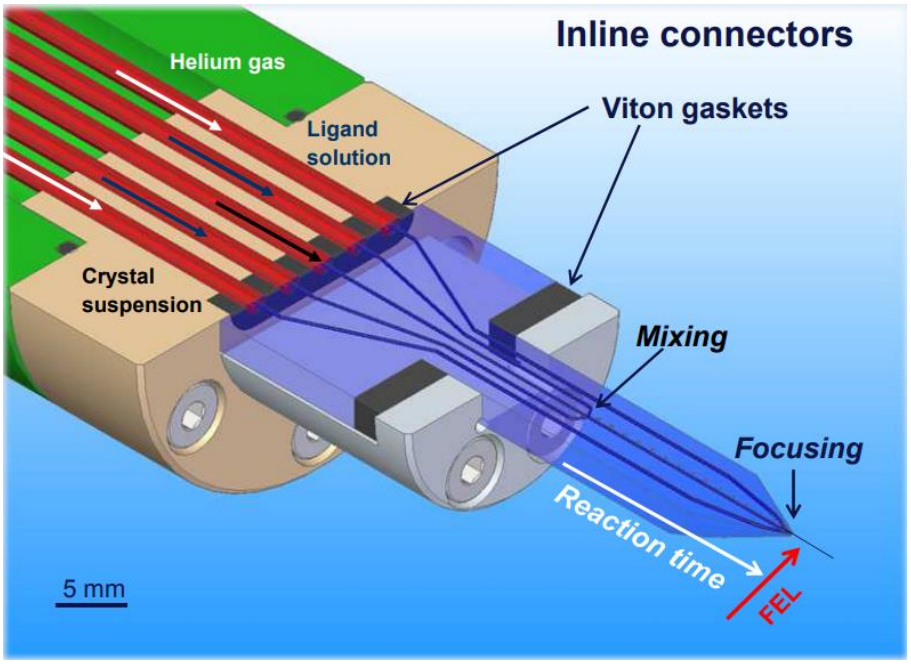

Figure 9. The GDVN device scheme.

3. Results

3.1. Preliminary experiments An aqueous suspension of 10 µm beads (2.5% (solids)) was loaded in a glass capillary of 500 µm I.D. (internal diameter) and 1000 µm O.D.(outer diameter) and imaged with bright field microscopy (Fig. 10a). The beads suspension was put on the glass plate and was dried. 200 mm camera lens was used for obtaining fluorescence image of 10 µm size beads in static condition (Fig..10b), and 300 mm camera lens was used for obtaining fluorescence image of 1 µm size beads (Fig.10c).

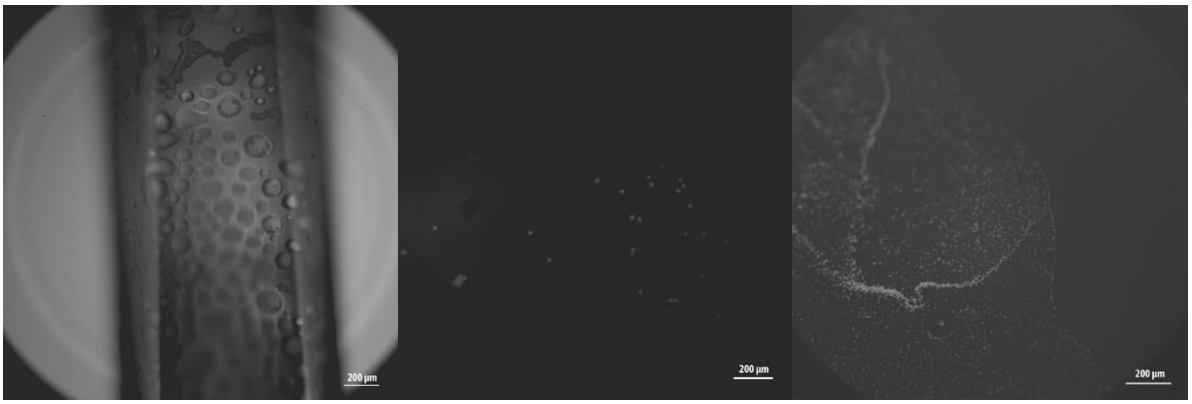

a) b) c)

Figure 10. a) 10 µm size beads imaged with bright field microscopy, b) Fluorescence image of dried droplet of 10 µm beads suspension on glass plate, c) Fluorescence image of dried droplet of 1 µm beads suspension on glass plate.

The data analysis was conducted via software ImageJ, which enables for continuous slow-motion process monitoring of long image sequences. The program performs background subtraction according to the set options to minimize baseline noise. The "Plot Profile" function of ImageJ program displays in the two-dimensional graph the pixel distribution intensity on the dedicated line. The ratio is 0.53 pixels/µm. 1 pixel=1.90 µm. The fluorescence intensity curve of liquid jet with Rhodamine 6G solution is presented in figure 11. The width of peak is 61 pixels. After dimensional transformation the diameter of liquid jet is 116 µm.

3.2. Liquid jet speed determination. Rhodamine 6G suspension was flushed through a nozzle with a flow rate of 0,2 ml/min, producing a liquid jet of diameter 116 µm (Fig. 11).

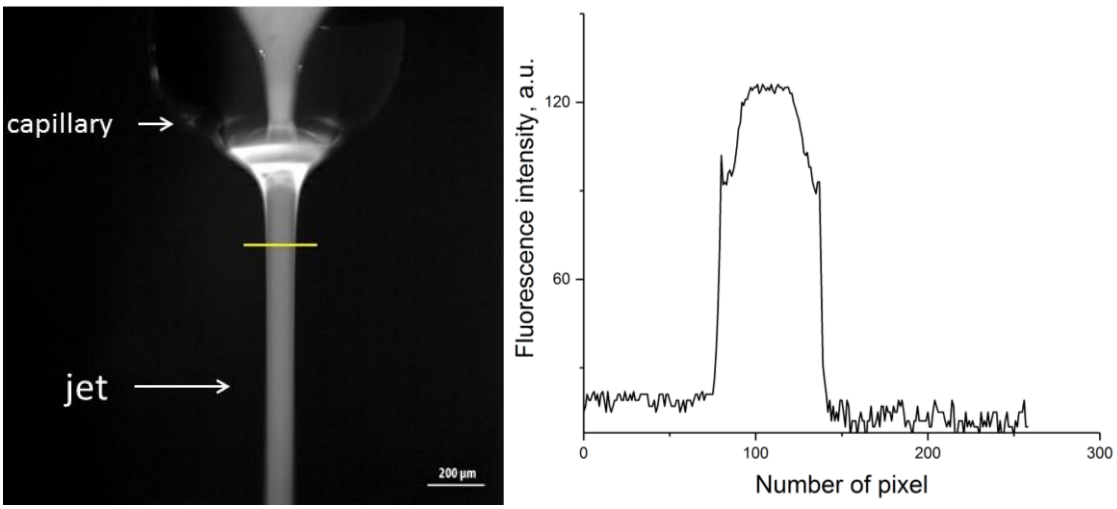

a) b)

Figure 11. a) Fluorescent image of Rhodamine 6G solution jet, b) Plotted intensity along the yellow line in (a).

Figure 12a shows a picture collected at LED double exposure mode, within the acquisition of a singleframe. A bead flowing in the jet aqueous suspension is visualized at two distinct time points, defined by the delay between the pulses and the synchronization with the camera acquisition. Such procedure allows measuring the distance covered by the moving bead in a given time and, therefore, calculating the jet speed. The threshold operation of ImageJ was used for red highlighting maximum intensity of beads. It highlights pixels which fall within a desired range of intensity values from those which do not. The fluorescence intensity graph was obtained via ImageJ Plot Profile function, along a line connecting the bead imaged at different time points. Origin program was used to localize the bead positions and therefore quantifying the bead and jet speed (Fig.. 12b).

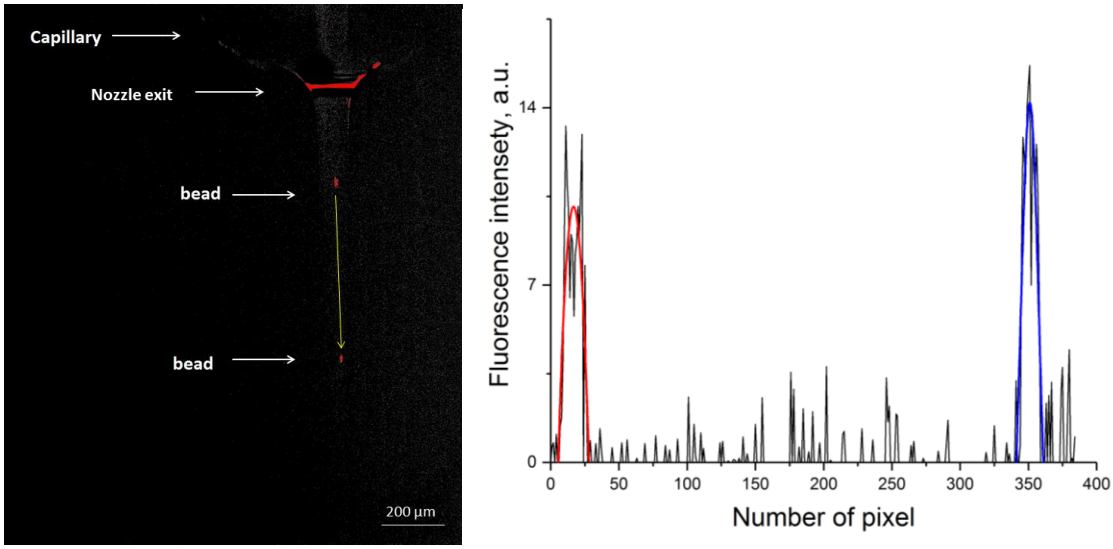

a) b)

Figure 12. a) Thresholded fluorescent image of 5 μm beads, b) Intensity profile along line connecting the twice imaged 5 μm bead.

The fluorescence intensity parts of the curve relative to the beads positions were fitted by Gaussian function. The first bead maximum intensity is observed at 17 unit of the pixel number axis. The second maximum peak observed at 351 unit of the pixel number axis. The distance between beads is 334 pixels, which corresponds to 635 μm. The delay time is 200 μs, consequently the speed of jet is 3.17. The same steps were done with 10 μm beads (Fig.13).

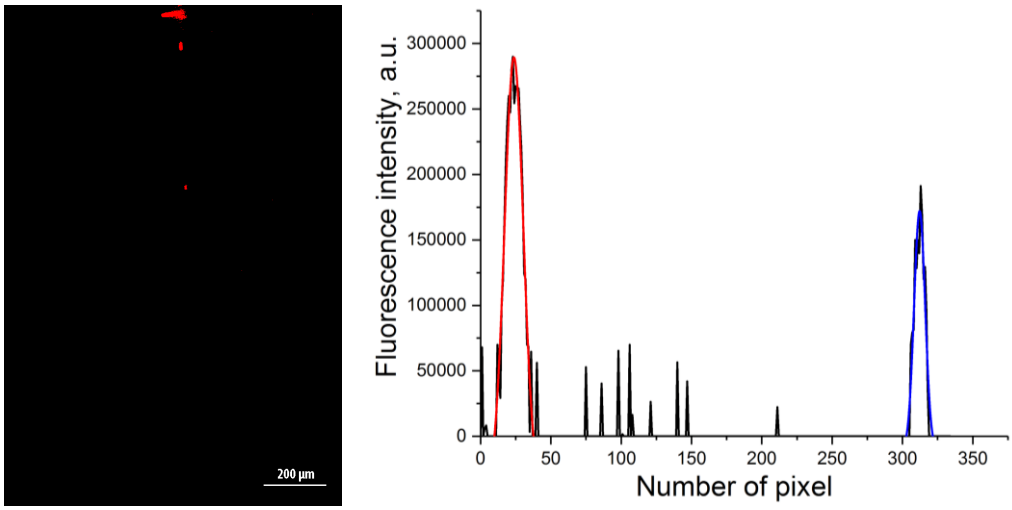

a) b)

Figure 13. a) The fluorescent image of 10 μm beads, b) dependency graph of 10 μm beads fluorescence intensity and number of pixel.

The first bead has maximum intensity at 24 unit of the pixel number axis. The second maximum peak observed at 312 unit of the pixel number axis. The distance between beads is 289 pixels, after calculation is 548 μm. Therefore, the jet speed is 2.7 m/s.

3.3. Mixing experiments.

The aim of the experiment was to characterize the mixing time of a custom-made glass micro-mixer. The geometry is shown in Fig. 9. The channel cross-section is 160μm x160μm. And the angle between the central channel and the lateral ones is 56°. In order to perform the task, fluorescence quenching of Rhodamine 6G dye via potassium iodide was observed. The method has been utilized by Calvey et al. [1] to characterize their mixing device. [19]. 20 μM Rhodamine 6G dye solution was injected through the central capillary and 300 mM potassium iodide through the outer coaxial capillary with flow rate ratios 1:40 and 1:30. The total flow rate was 62 μl/min. After 0.25 ms the fluorescence decreased by half, and after 1 ms its minimum level was achieved in both cases.

At first, the final and initial states of the fluorescence quenching reaction of Rhodamine 6G due to potassium iodide were imaged (Fig.14).

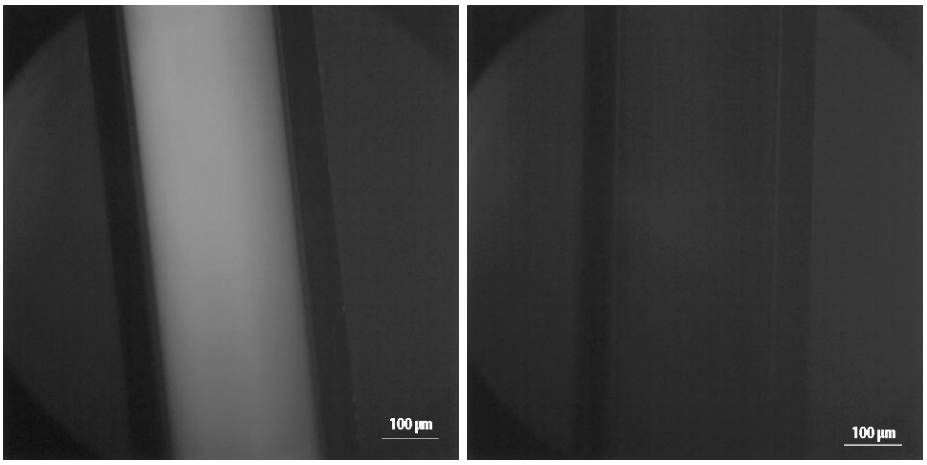

a) b)

Figure 14 . Fluorescence image of a) the capillary with 20 µM Rhodamine 6G, b) the capillary with 300 mM potassium iodide.

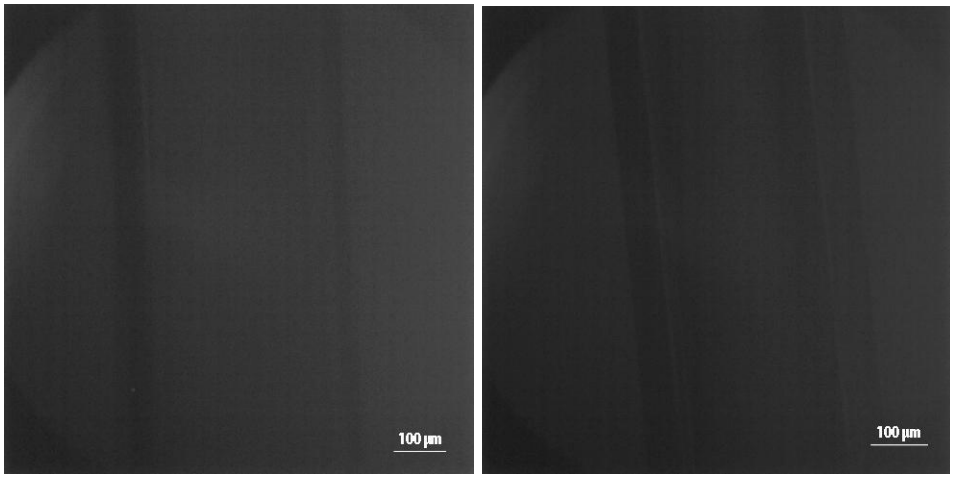

a) b)

Figure 15. Fluorescence images of Rhodamine 6G and potassium iodide mixed solutions a) with ratio 1:1, b) with ratio 1:2.

In Fig.14 you can notice the fluorescence of Rhodamine dye and the non-fluorescence of potassium iodide. After reagents mixing with 1:1 ratio fluorescence is not observed anymore. The same result was obtained with ratio 1:2 of Rhodamine 6G and potassium iodide respectively. (Fig. 15)

To characterize the mixing process in the microfluidic device, we flowed 20 µM Rhodamine dye through the inner channel with 5.0±0.1 µl/min flow rate and 300 mM potassium iodide in the two outer channels with 80±2 µl/min flow rate. Finally, the total rate was 165±5 µl/min (Fig. 16).

a) b)

Figure 16. a) The fluorescence image of Rhodamine 6G and potassium iodide mixing, b) the fluorescence image of Rhodamine 6G and potassium iodide mixing with red highlighting of fluorescence quenching.

The Rhodamine 6G fluorescence is observed during 978 µm. The device channels have square shape with 160 µm side. Consequently, channel volume with Rhodamine fluorescence quenching is 17.51 pm^3 or 25.05 nl. The mixing speed can be measured via these values:

$$Velocity = \frac{Distance \times Flow\ rate}{Volume} \quad (1)$$

$$Time = \frac{Volume}{Flow\ rate} \quad (2)$$

$$Velocity = \frac{Distance}{Time} \quad (3)$$

The mixing time of Rhodamine 6G and potassium iodide is 9.4±0.3 ms and mixing speed is 104±3 mm/s.

The experiment was afterwards repeated with 10 µm beads flowing through the central channel to validate the speed measuring procedure. The Rhodamine B beads were flowed through the inner channel with 5.0±0.1 µl/min flow rate and water was flowed through each of two outer channels with 80±2 µm/min flow rate (Fig. 17). The results were registered via streak camera and LED double pulse mode. The pulses width were 10.00±0.01 µs and delay between pulses was 200.00±0.01 µs µs. Axial distances down the flow in central upper channel, before the point of two streams join and lower channels after the point where the two streams join were measured by this method, and then liquid jet speeds in different channels of the device were calculated.

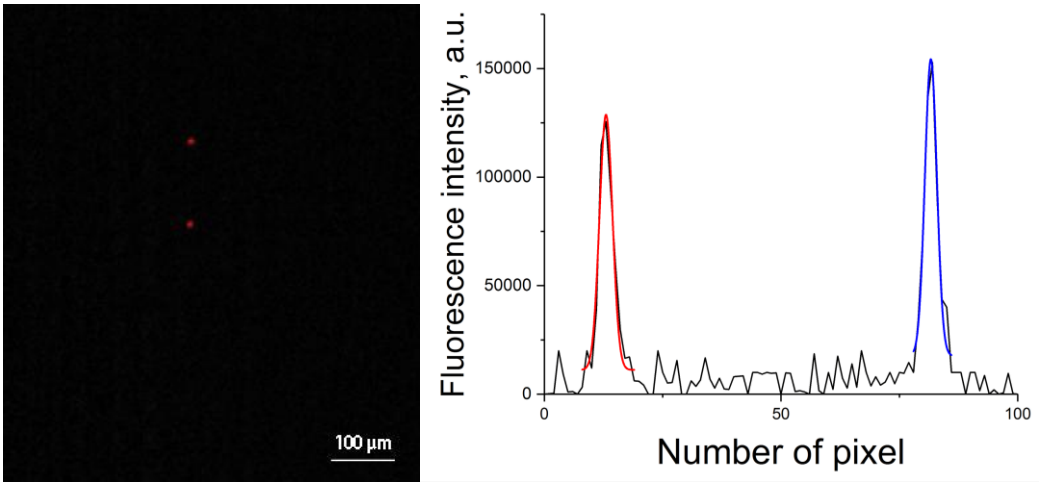

a) b)

Figure 17. a) The fluorescent image of 10 µm beads in central upper channel of the device, b) dependency graph of 10 µm beads fluorescence intensity and number of pixel in central upper channel of the device.

The first bead maximum intensity peak is observed at 13 unit of the pixel number axis, the second peak is observed at 82 unit of the pixel number axis. Consequently, the distance between peaks is 69 pixels or 130 µm. The liquid jet speed in central upper channel before mixing point is 6.52±0.05 mm/s.

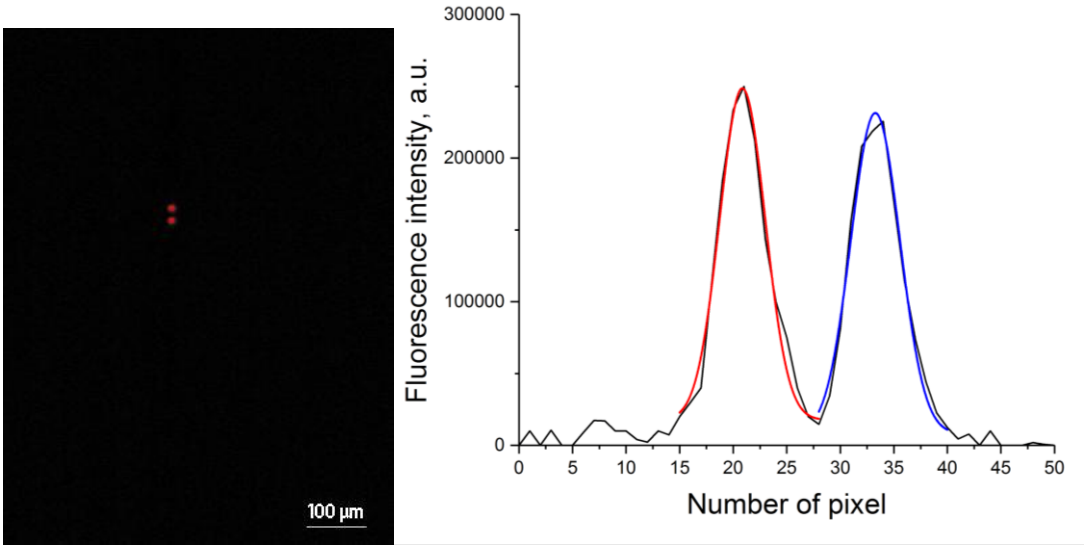

a) b)

Figure 18. a) The fluorescent image of 10 µm beads in the device channel after jets mixing, b) dependency graph of 10 µm beads fluorescence intensity and number of pixel in in channel after jet mixing of the device.

The first bead maximum intensity peak is observed at 21 unit of the pixel number axis, the second maximum intensity peak is observed at 33 unit of the pixel number axis. In the device channel after mixing (Fig. 18a)the distance between peaks is 12 pixels or 24 μm. Therefore, the jet speed is 118±1 mm/s.

3.3.1. The diffusion coefficient calculation. The following expression has been used to calculate the diffusion coefficient [1]:

$$D = \frac{d^2}{t} \qquad (4)$$

where *d* is sample diameter, *t* is mixing time. The sample diameter in average is 5.1±0,3 pixels or 93±0,5 μm and consequently *D*= 9.3±1,3 mm^2/s.

a) b) c)

Figure 19. a) Fluorescence image of Rhodamine 6G (10 μl/min)and potassium iodide (150 μl/min) at the beginning mixing, b) the fluorescence image of Rhodamine 6G and potassium iodide at the finishing mixing, c) the fluorescence image of Rhodamine 6G and potassium iodide mixing with red highlighting of fluorescence quenching.

The diffusion coefficient was calculated for mixing of Rhodamine 6G and potassium iodide, which Rhodamine 6G flow rate in central channel was 10,0±0,3 μl/min and potassium iodide flow rate was 150±5 μl/min and total flow rate is 310±9 μl/min. The images were registered at the beginning mixing and finishing fluorescence quenching due to the small camera aperture (Fig. 19). The distance between symbols etched into the glass device is 1 mm. The distance between mixing point and the first symbol is 1.2 mm. The distance between mixing point and symbol from picture is 5.2 mm. Consequently, the Rhodamine 6G and potassium iodide mixing distance is 5386 μm. Mixing time is 12.4±0.04 ms. Diffusion coefficient is D=7.7±1.2 mm^2/s.

3.4. The fluorescence intensity of liquid jets with different speeds. The analysis of the fluorescence intensity for the Rhodamine 6G and potassium iodide mixing was conducted via Matlab software. The 8 points were chosen in fluorescence image. The first point corresponds

to the mixing point of solutions. The time between points is 1 ms, which was calculated via formulas in the Matlab script (Figure 20). Firstly the fluorescence image of Rhodamine 6G and potassium iodide was chosen with solution rate ratios 1:32 and total flow rate 165±5 µl/min.

The Rhodamine 6G and potassium iodide intensity plots at different time points are presented on the figures 21 and 22.

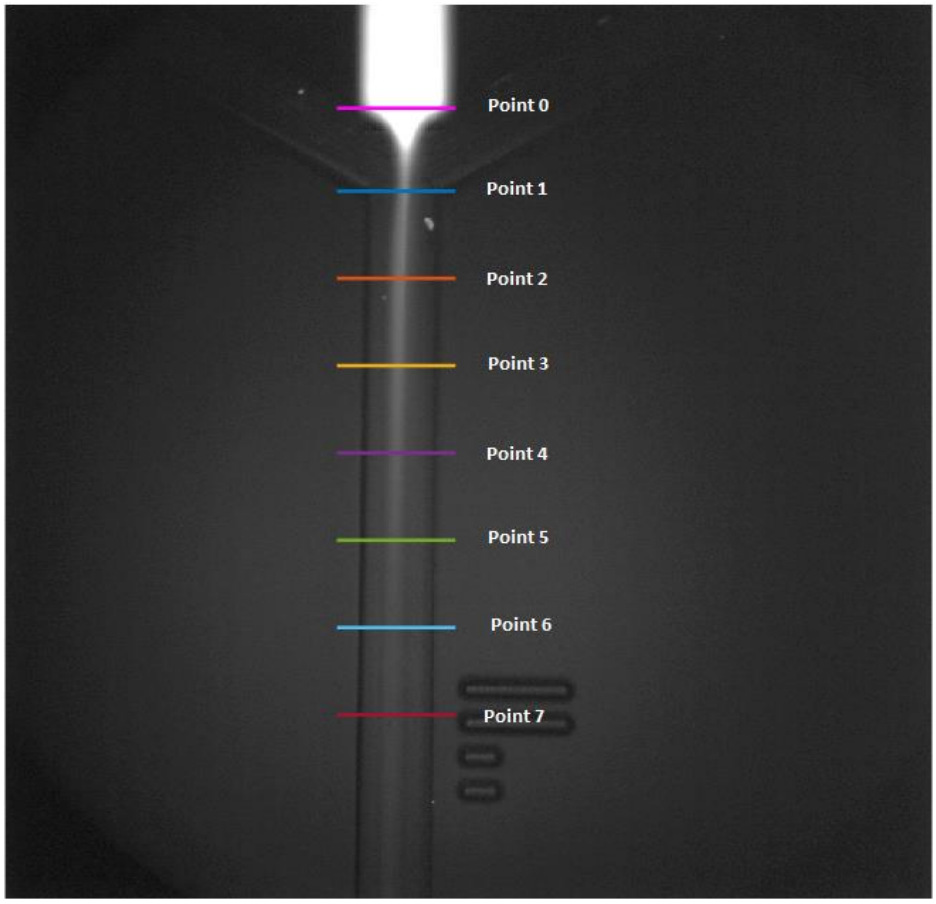

Figure 20. The fluorescence image of Rhodamine 6G (5µl/min)and potassium iodide(80/µl/min, for each inlets).

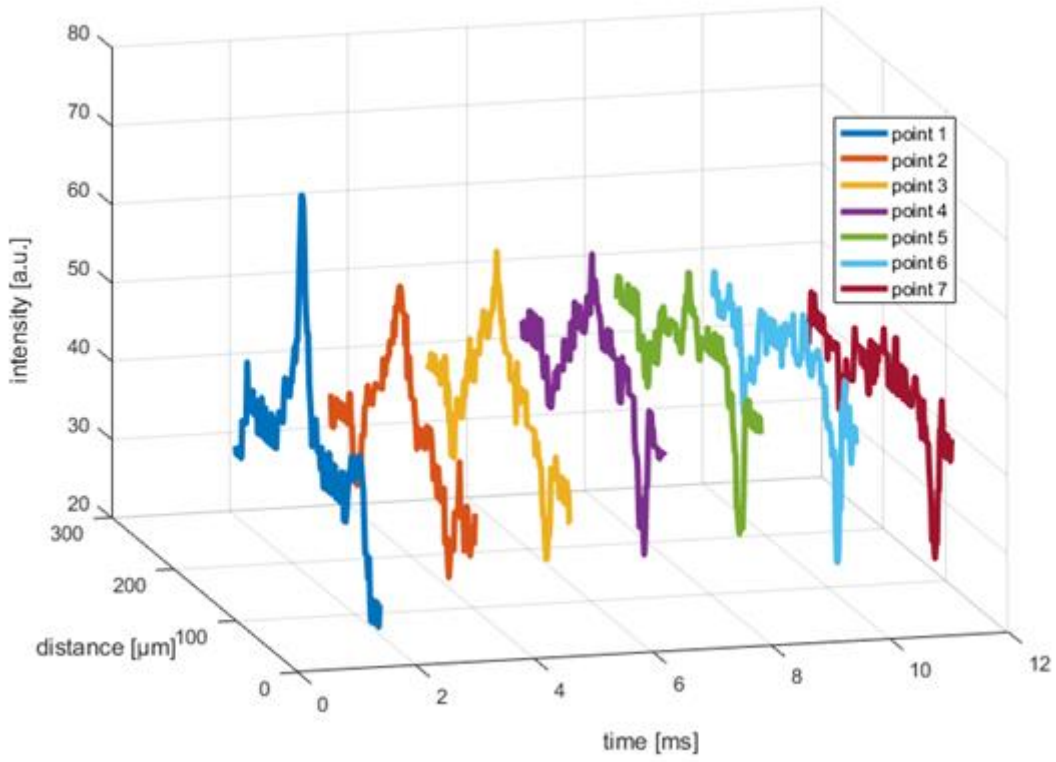

Figure 21. The Rhodamine 6G and potassium iodide intensity plots at different time points.

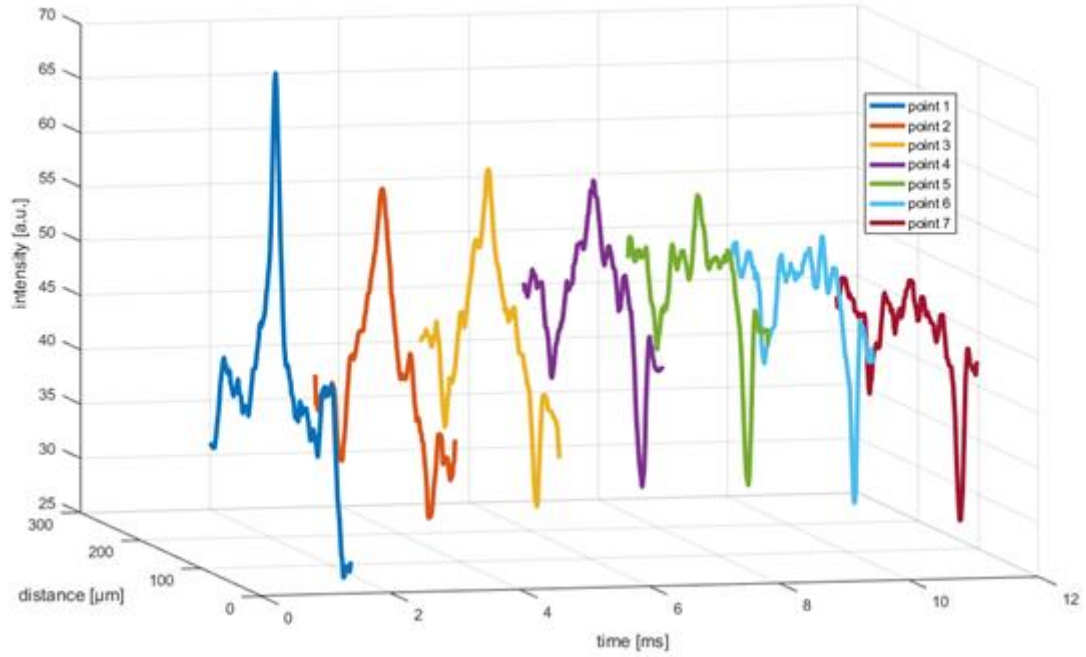

Figure 22. The Rhodamine 6G and potassium iodide intensity plots at different time points after smoothing.

On the figure 22 the plots have been smoothed by a function that uses a moving average filterto decrease the data noise. The lowest points correspond with the edges of channel. The

same steps were conducted for Rhodamine 6G and potassium iodide was chosen with solution rate ratios 1:30 and total flow rate 310±9 µl/min (figures 23-25).

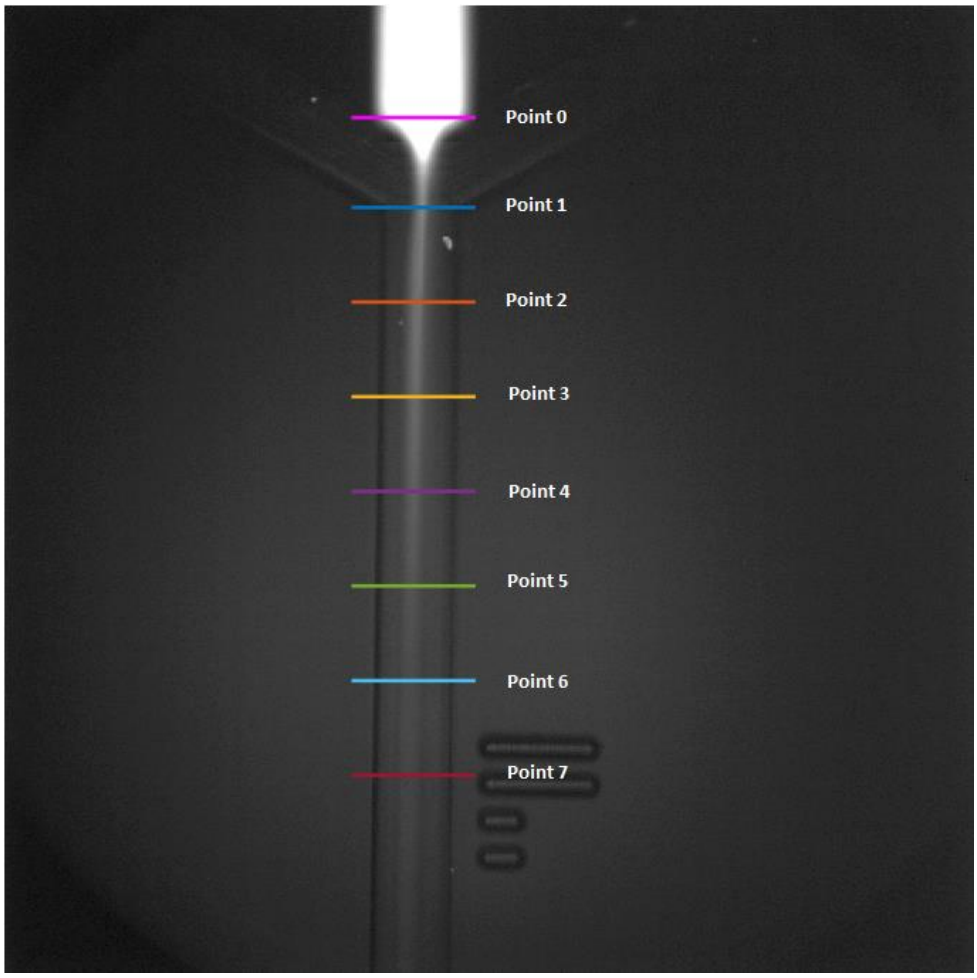

Figure 23. The fluorescence image of Rhodamine 6G and potassium iodide. The total flow rate was 310µl/min..

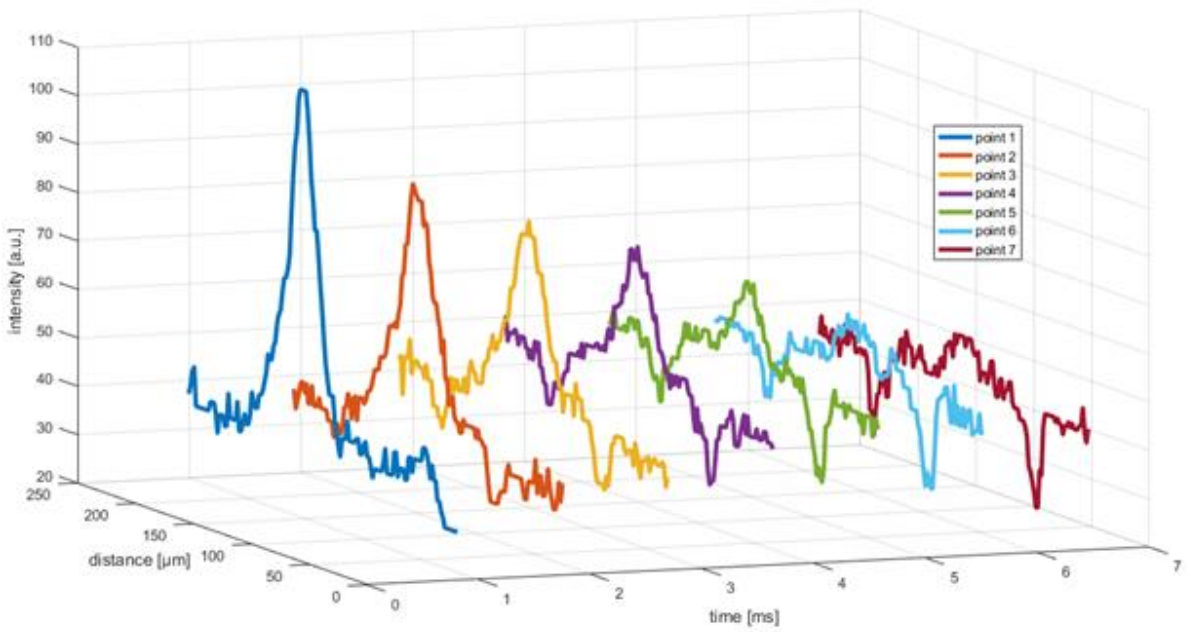

Figure 24. The Rhodamine 6G and potassium iodide intensity plots at different time points.Total flow rate 310 µl/min.

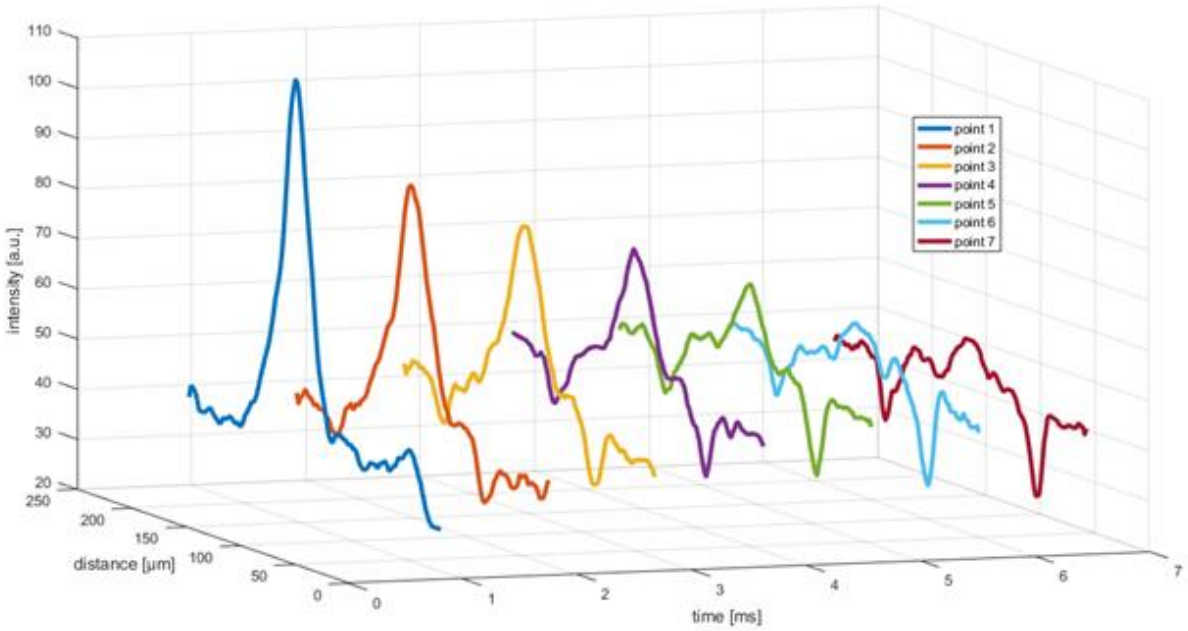

Figure 25. The Rhodamine 6G and potassium iodide intensity plots at different time points after smoothing. Total flow rate 310 µl/min.

The fluorescence intensities of Rhodamine 6G and potassium iodide mixing were compared with different values. In the first case the solution rate ratio was 1:32 and total flow rate was 165±5 µl/min. On the second case the flow rate ratio and total flow rate were 1:30 and 310±9 µl/min respectively.

4. Conclusion

During this work the set-up for protein conformation studies was assembled and calibrated. Experimentally, the delays between pulses and its width were selected for LED pulse mode. Also LED pulse mode was synchronized with camera shutter for registration sequence of flowing Rhodamine B beads. The experiments with the mixing device characterized the mixing times at different flow rates. The rapid fluorescence quenching was observed with the same solution concentrations from Calvey experiments with solution rate ratios 1:32 and total flow rate 165±5 μl/min. The full fluorescence quenching was observed after 9.4±0.3 ms. Also the diffusion coefficient was measured in the two cases. At the first case flow rate ratio was 1:32 and total flow rate was 165±5 μl/min, and the second case flow rate ratio 1:30 and total flow rate was 310±9 μl/min. The diffusion coefficients are 9.3±1.3 mm^2/s and 7.7±1.2 mm^2/s, respectively. The first calculated value lies within the error function of the second value.

The faster flow rate provide better fluorescence intensity decline for analysis.

The set-up developed for performing these experiments will allow tracking structural changes of valuable samples. The characterization of the jet speed and the mixing time of the device will provide important information for future experiments at European XFEL.

Acknowledgements

I would like to give sincere thanks to my supervisor Rita Graceffa and Sample Environment group of European XFEL. They gave me good advices, support and feedback throughout this project in the framework of the DESY Summer Student Program. Also I would like to thank all the DESY Summer Student Program 2017 organisers for allowing me to experience this program.

References

1. Calvey G.D., Kartz A.M., Schaffer C.B., Pollack L. Mixing injector enables time-resolved crystallography with high hit rate at X-ray free electrons lasers // Structural Dynamics, vol. 3, issue 5, 2016, article number 054301.
2. Wang D., Weierstall U., Polack L., Spence J. Double-focusing mixing jet for XFEL study of chemical kinetics // Journal of Synchrotron Radiation, vol. 21, part 6, 2014, pp. 1364-1366.
3. Moffat K. Time-Resolved Macromolecular Crystallography // Annual Review of Biophysics and Biophysical Chemistry, vol. 18, 1989, pp. 309-332.
4. Schmidt M. Structure Based Kinetics by Time-Resolved X-ray Crystallography // Biological and Medical Physics, Biomedical Engineering (Springer), 2008, pp. 201-241.

5. Schmidt M. Mix and inject: Reaction initiation by diffusion for time-resolved macromolecular crystallography // Advances in Condensed Matter Physics, 2013, Article number 167276.
6. Schotte F., Lim M.H., Jackson T. A., Smirnov A. V., Soman J., Olson J. S., Phillips G. N., Wulff M., Anfinrud P. A. Watching a protein as it functions with 150-ps time-resolved x-ray crystallography. // Science, vol. 300, issue, 2003, pp. 1944–1947.
7. Genick U. K., Borgstahl G. E. O., Ng K., Ren Z., Pradervand C., Burke P. M., Srajer V., Teng T., Schildkamp W., McRee D. E., Moffat K., Getzoff E. D. Structure of a protein photocycle intermediate by millisecond time—Resolved crystallography. // Science, vol. 275, issue 5305, 1997, pp. 1471–1475.
8. Geremia S., Campagnolo M., Demitri N., Johnson L. N. Simulation of diffusion time of small molecules in protein crystals // Structure, vol. 14, issue 3, 2006, pp.393–400.
9. Hajdu J., Acharya K.R., Stuart D.I., Mclaughlin P.L., Barford D., Oikonomakos N.G., Klein H., Johnson L.N. Catalysis in the crystal: Synchrotron radiation studies with glycogen phosphorylase b // EMBO Journal, vol. 6, issue 2, 1987, pp.539–546.
10. Stagno J.R., Liu Y., Bhandari Y.R., Conrad C.E., Panja S., Swain M., Fan L., Nelson G., Li C., Wendel D.R. Structure of Riboswitch RNA Reaction States by Mix-and-Inject XFEL serial Crystallography. // Nature, vol. 541, issue 7636, 2017, p. 242-249.
11. Stan C.A., Milathianaki D., Laksmono H., Sierra R.G., McQueen T.A., Messerschmidt M., Williams G.J., Koglin J.E., Lane T.J., Hazes M.J. Liquid explosions induced by X-ray laser pulses. // Nature Physics, vol. 12, issue 10, 2016, pp. 966-971.
12. Weierstall U. Liquid sample delivery techniques for serial femtosecond crystallography // Philosophical Transactions of the Royal Society B-Biological Science, vol. 369, issue 1647, 2014, Article number 20130337.
13. DePonte D. P., Weierstall U., Schmidt K., Warner J., Starodub D., Spence J. C. H., Doak R. B. Gas dynamic virtual nozzle for generation of microscopic droplet streams // Journal of Physics D-Applied Physics, vol. 41, issue 19, 2008, Article number 195505.
14. Ganan-Calvo A.M., Generation of steady liquid microthreads and micron-sized monodisperse sprays in gas streams // Physical Review Letters, vol. 80, issue 2, 1998, pp. 285–288.
15. Herrada M. A., Ganan-Calvo A. M., Ojeda-Monge A., Bluth B., Riesco-Chueca P. Liquid flow focused by a gas: Jetting, dripping, and recirculation // Physical Review E, vol. 78, issue 3, part 2, Article 2008, number 036323.
16. Nelson G., Kirian R.A., Weierstall U., Zatsepin N.A., Farago T., Baumbach T., Wilde F., Niesler F.B.P., Zimmer B., Ishigami I. Three-dimensional-printed gas dynamic virtual nozzles for X-ray laser sample delivery // Optic s Express, vol. 24, issue 11, 2016, p. 1515-1530.
17. Hardware Manual “Fastcam SA4 FASTCAMSA4 RV” // PHOTRON LIMITED, 2014, p. 15.

18. IL-104X IL-105X IL-106X High-Power-LED Illuminators for pulsed and continuous operation // HARDsoft Microprocessor System, Licensed by DLR German Aerospace Center, 2011, p.
19. Knight J., Vishwanath A., Brody J., Austin R., Hydrodynamic focusing on a silicon chip: Mixing nanoliters in microseconds // Physical Review Letters, vol. 80, issue 17, 1998, pp. 3863–3866.